RSC Advances

PAPER

View Article Online
View Journal | View Issue

Cite this: *RSC Adv.*, 2024, **14**, 39131

Stability and performance investigation using different electrode configurations and electrolyte compositions in an oxyhydrogen gas generator†

Waqas Mughal, *[ab] Pei Ji, *[a] Usman Rauf,[b] Liu Junping,[a] Abdul Waheed[b] and Perdeep Kumar[b]

This study aimed to develop an efficient HHO generator with higher gas production, enhanced electrodes, and stable current density. For HHO generator stack fabrication, 15 plates of 304L stainless steel were utilized, accompanied with a 4 mm rubber separator to maintain the gap between electrodes. Each plate in the stack was connected *via* a separate wire through lug spot welding, enabling the assembly of different configurations for testing. The study introduced three distinct configurations: in the first configuration, no neutral plate was used between the electrodes; the second incorporated one neutral plate; and the third configuration utilized six neutral plates between the cathode and anode. These configurations were tested at 2, 4, and 6 g per L KOH concentrations. In addition, the HHO generator was tested using the pulse width modulation (PWM) approach to adjust voltages at different levels. According to the results, Configuration-2 produced the most significant amount of oxyhydrogen gas with KOH concentrations of 4 and 6 g L^{-1}. Further examination showed that the gas production was unstable when the generator operated continuously for 10 hours, displaying a consistent decrease over time. However, when tested at 2 g L^{-1} concentration, the yield was slightly lower but more stable. Additionally, it was observed that in Configuration 1, applying higher voltage and current to each cell in the stack led to the formation of iron oxide, resulting in a significant 43% drop in current density in the first 10 hours, which reached 65% after 10 days. In this study, a mathematical model was developed to predict the electric conductivity of the prepared aqueous electrolytic solution of KOH at different temperatures, along with a mathematical model for predicting HHO gas production at different voltages, KOH concentrations and electrode arrangements.

Received 2nd November 2024
Accepted 27th November 2024

DOI: 10.1039/d4ra07816k

rsc.li/rsc-advances

1. Introduction

The growing need of fossil fuels and the substantial production of harmful pollutants have directed us toward exploring renewable alternative fuels.[1] The 2022 World Air Quality Report indicates that India ranks as the eighth most polluted country, exhibiting a PM2.5 value of 53.3 μg m^{-3}.[2] The emission of Carbon dioxide into the atmosphere by industries and sectors such as automotive manufacturing, transportation, and power generation, and it plays a significant role in deteriorating the environment. As a source of energy, these sectors rely on the combustion of hydrocarbon fuels, which contributes to global warming, air pollution, and the depletion of fossil fuel reservoirs. Furthermore, these components endanger human health.[3] As a significant environment-friendly renewable energy source, hydrogen shows promise in satisfying the world's growing energy needs.[4] Hydrogen has the potential to replace fossil fuels in a significant way. Its combustion and emission properties are better than those of hydrocarbon fuels. There are some possible raw materials such as biomass, coal, and water are used for its production. The main benefit of utilising hydrogen as a fuel is the reduction of flue gas emissions. The combination of hydrogen and oxygen is commonly known as oxyhydrogen or brown gas.[3] Water electrolysis is the most favorable technique for generating oxyhydrogen gas (HHO), also known as green hydrogen.[5] An electrolytic cell facilitates the decomposition of water into its constituent gases, hydrogen and oxygen, where hydrogen is generated at the cathode and oxygen at the anode.[6] HHO gas is generated through electrolysis and enhances the oxygen supply for combustion.[7] However, the primary objective is to reduce energy consumption while simultaneously enhancing the production of HHO gas.[8] HHO has unique combustion characteristics, including an extra-wide flammability range from 5% to 74%, a flame speed of 3200 meters per second, and combustion of both in the pre-mixed

[a]*Research Center of Fluid Machinery Engineering and Technology, Jiangsu University, Zhenjiang 212013, China. E-mail: Engr.pirbux@outlook.com; jpei@ujs.edu.cn*
[b]*Department of Mechanical Engineering, Quaid-e-Awam University of Engineering, Science and Technology, Nawabshah, Sindh, Pakistan*

† Electronic supplementary information (ESI) available. See DOI: https://doi.org/10.1039/d4ra07816k

and diffusion modes.[9,10] The design, development and implementation of effective electrocatalysts for the electrochemical reduction and oxidation of water are crucial to attaining the breakthrough of hydrogen energy from marginal energy sources for large-scale applications.[11] Santilli developed a system consisting of an anode, cathode, DC power source, and an electrolyte solution to produce HHO gas. Electric current facilitates the dissociation of water molecules into hydrogen and oxygen ions. This process, known as electrolysis, produces hydrogen at the cathode and oxygen at the anode. Adding electrolyte solutions, such as KOH and NaOH, to pure water is essential due to its inherently low electrical conductivity. By incorporating these substances, the ionic concentration in water increases, thereby enhancing its ability to conduct electricity. HHO gas, often referred to as oxyhydrogen, is a composite mixture consisting of oxygen and hydrogen atoms, their dimeric forms, such as H_2O_2, alongside separate molecules of oxygen (O_2) and hydrogen (H_2), as well as residual, unreacted water molecules.[12] In a study on dry cells, Olivares *et al.* examined the performance of three distinct stainless-steel grades, 304L, 316L, and 430L, in conjunction with different concentrations of KOH and NaOH solutions. Among the materials evaluated, stainless steel 316L emerged as the most effective cathodic electrode in an alkaline environment composed of KOH.[13] Yilmaz *et al.* investigated the generation rate of oxyhydrogen gas in a wet cell by using an electronic control unit and comparing several electrolyte solutions, such as NaOH, NaCl, and KOH.[14] Arjun *et al.* researched the impact of HHO gas on engine performance and emisison.[15] Musmar *et al.* investigated the generation rate of HHO gas in a wet cell, using Na_2CO_3 as the electrolyte and stainless steel as the electrode material.[16] Sudarmanta *et al.* and De Silva dedicated their efforts to improving the efficiency of an oxyhydrogen generator by incorporating the pulse width modulation (PWM) duty cycle technique into their design.[17,18] Mazloomi *et al.* offered insights into several factors for reducing energy losses in the water electrolysis process within a dry cell. They investigated different parameters, such as electrolyte electrical resistance, electrolyte concentration, temperature, spacing between the electrodes, electrode material, applied voltage, and electrode alignment. Water electrolysis efficiency was enhanced through a comprehensive study of the physical, chemical, and electrical properties.[19] Shashikant *et al.* detailed an experimental optimization process involving parameter design by utilizing the Taguchi optimization method. They applied this method to enhance HHO production with various grades of stainless-steel electrodes while using HNO_3 and Na_2CO_3 electrolytes. The flow rate of HHO was influenced by factors such as electrolyte concentration, electrolytic time, and applied current.[20] Bahlake *et al.* conducted a study on temperature and electrolyte optimization by applying a response surface methodology. They aimed to maximize the produced voltage, which served as the response function. This maximization was achieved by adjusting parameters such as the cathode type, electrolyte, and system temperature. Through this approach, they developed an optimal electrochemical cell by considering the influence of each factor and determining their optimal values.[21] Polverino *et al.* investigated the energy characteristics associated with oxy-hydrogen production. They categorized electrolyzers into electrolyte membrane, polymer, alkaline, and solid and focused on ensuring that the energy needed to produce HHO remained below the engine's efficient energy consumption.[22] Masjuki *et al.* study examines alkaline water electrolysis for HHO gas production in a biodiesel-fueled diesel engine. Stainless steel electrodes and KOH electrolyte were used in atmospheric pressure for production of HHO gas.[23] Al-Rousan investigated how the spacing between cathode and anode plates in HHO cells impacts engine performance and emissions.[24] Subramanian *et al.* demonstrated that an increase in electrolyte concentration resulted in higher conductivity and reduced the electric potential.[3] Elgarhi *et al.* provided evidence that a dry cell with four anodes and four cathodes using KOH as the electrolyte exhibited high resistance to corrosion, primarily due to the potassium content. They found that 6 g L^{-1} of KOH concentration improved the HHO cell performance.[25] Electrode stability is an important factor in maintaining the performance and service life of electrochemical systems, such as HHO gas generators, fuel cells, and batteries, which guarantee consistent and better electrical performance and lead to reliable production rates and energy efficiency. Stable electrodes without degradation in HHO generators prevent fluctuations in current density and reduce the risk of overheating or abnormal gas production. There have been several research works on improving the yield of oxyhydrogen gas, as given in Table 1. Nonetheless, very limited literature has been found on the stability of the entire stack of the oxyhydrogen gas generators.

Table 1 Comparison of HHO yield obtained from literature findings

Sr.	Type of cell	Electrode	Electrolyte	Concentration (grams)	Applied voltages	Current (amp)	HHO yield (LPM)	Reference
1	Dry	SS316L	NaOH	4–20	2–11	6–42	0.86–1.09	26
2				20	12	20	0.5	27
3				5	2–5	14	0.86	28
4	Wet			20	12	35	0.6	29
5				100	12	25	0.5	30
6				20	12	35	0.75	27
7				1.2	—	15	0.9	27
8				10	5–11	17.8	1.16	28
9			KOH	5.61	3–10	2	0.1	27

This research investigated the stability of HHO cells with electrode gaps of 4 mm by using 15 electrodes and employing three distinct electrode configurations. In HHO generators, the relationship between the electrode gap and electrolyte concentration can be a complicated phenomenon because both factors affect the efficiency of the electrolysis process. The electrolysis process for gas production was facilitated using potassium hydroxide (KOH) electrolyte at concentrations of 2, 4 and 6 g L^{-1}, which are approximately equal to 0.03565, 0.0713, and 0.10694 mol L^{-1}, respectively. Our study focused on understanding the performance and stability of the HHO cell under varying electrolyte concentrations and three different electrode configurations, aiming to provide insights into the optimal conditions for efficient gas production through electrolysis. There is very limited literature on the development of mathematical models to predict HHO gas production at different voltages and electrolyte concentrations. In this study, a mathematical model has been developed to predict HHO gas production at different voltages, concentrations, and electrode arrangements. Another model was developed to predict the electric conductivity of the prepared aqueous electrolyte solutions of KOH at different temperatures.

2. Materials and methodology

The formation of HHO gas can be significantly affected by various factors, such as the type and concentration of the electrolyte, applied current, temperature during the gas production, voltage, number of plates, and the gap between electrodes. Numerous studies have explored the significant influence of design modifications on HHO production, specifically about consuming less current and voltages, reducing electrolyte concentration, and using a minimal number of plates.[8,16,31]

2.1 Experimental setup

In this study, the HHO gas was produced through a water electrolysis process. The two electrodes in electrolyzers are designated as the cathode (+) and the anode (−). Hydrogen is formed at the cathode (+) side of the plate, while oxygen is generated at the anode (−) side of the plate. Ionic compounds conduct electricity due to the unrestricted mobility of ions. After melting, ions can migrate inside an aqueous solution following the dissolution process in water or within a liquid state. The material that has been completely dissolved is referred to as an electrolyte.

The electrolyzer developed in this research features electrodes with dimensions of 152.4 × 152.4 mm and a thickness of 1 mm. The electrolyzer was fabricated using 304L stainless steel due to its robustness and anti-corrosion properties, ensuring it consistently upholds its structural integrity across the experimental stages. Oxyhydrogen generators are commonly made of 304L stainless steel due to their cost-effectiveness and corrosion resistance. 316L is resistant to chloride-induced corrosion, although HHO generators work in alkaline or neutral electrolytes, where corrosion is less severe than in marine or very acidic settings. 304L resists electrolysis-induced oxidation and corrosion, especially in mild electrolytes. 304L is cheaper than 316L, making it a better HHO generator building material because most consumers may not see the performance benefits. Unless the generator is severely corrosive, 304L is a cheaper and better material for these situations. A total of 15 electrodes were employed to develop three distinct configurations, as illustrated in Fig. 1. Attaching wire lugs to opposite corners of electrodes through spot welding significantly improves the wire connection process and simplifies the assembly of different electrode configurations. This method enhances the ease of connecting wires and streamlines the construction of various electrode designs. As a result, it substantially increases the efficiency and flexibility of the structural design of the electrolyzer. This approach is crucial in simplifying the construction and improving the performance and versatility of the electrolyzer systems.

The electrodes are effectively isolated using a 4 mm rubber separator in these setups. The rubber separator is essential to ensure insulation, reduce the possibility of electrical short circuits, and prevent electrolyte leaking from the electrolyzer. This research evaluates the performance of the electrolyzer by employing the pulse width modulation (PWM) technique, examining its impact in three different configurations. This study presents three new electrolyzer arrangements, each distinguished by the unique usage of neutral plates. Configuration-1 has no neutral plate (7P8NX0), but in

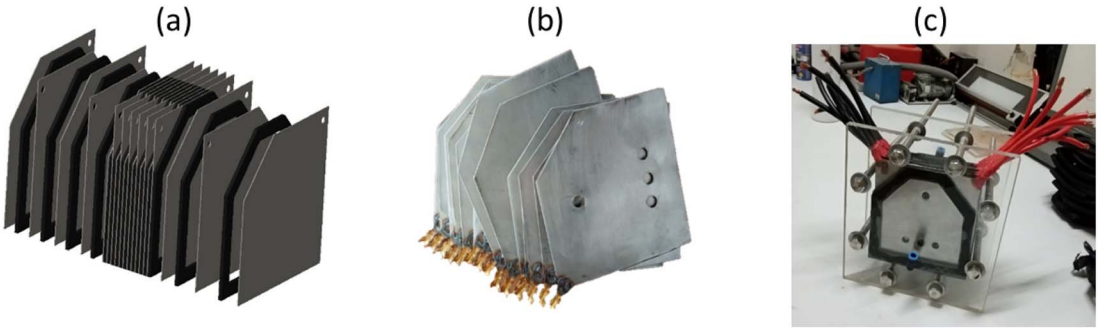

Fig. 1 (a) 3D-model of the HHO generator electrodes, (b) wire lugs spot-welded on electrodes and (c) complete assembled view of the HHO generator.

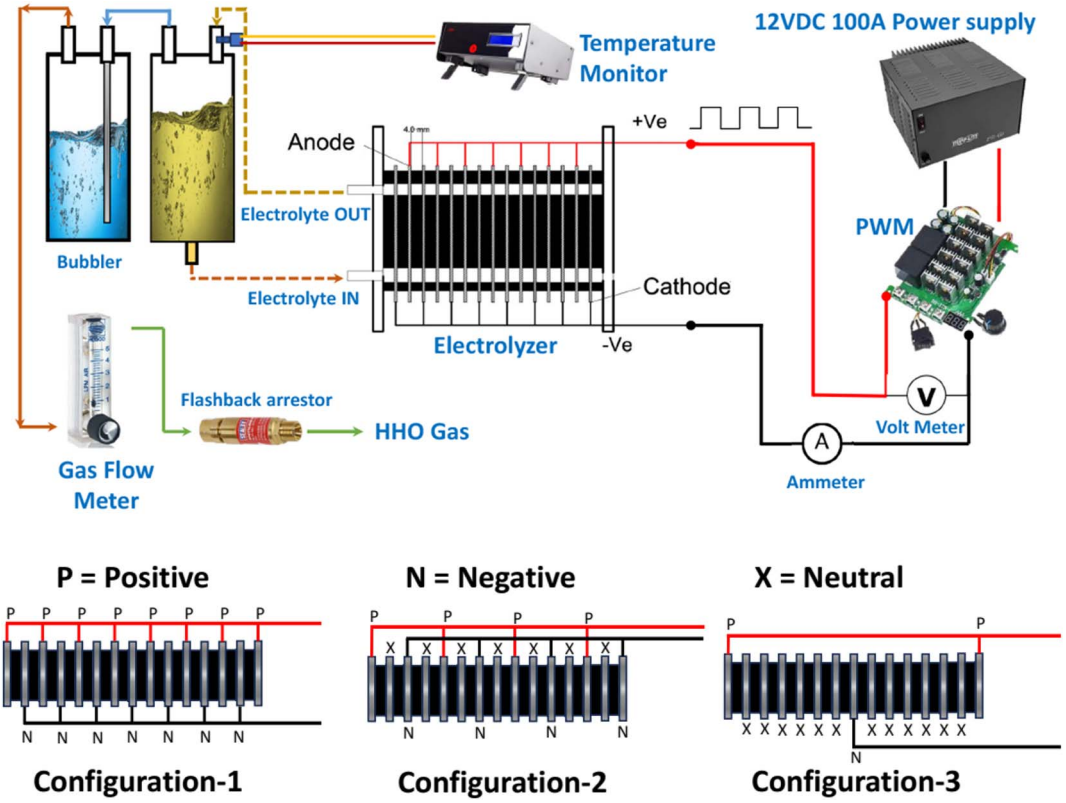

Fig. 2 Schematic of the experimental setup and electrode configurations.

Table 2 Instrument range and uncertainty in this study

Sr.	Instruments	Range	Resolution	Uncertainty
1	Voltmeter	0–30 VDC	0.1 volt	±0.2%
2	Ammeter	0–100 amp	0.1 amp	±0.2%
3	Thermocouple (K-type)	−200–1260 °C	0.1 °C	±0.75%
4	Timer	0–24 h	0.001 s	±0.1%
5	Electronic balance	10–1000 mg	10 mg	±0.1%
6	Gas flow meter	0.5–5 L min^{-1}	0.5 L min^{-1}	±5%

Configuration-2, one neutral plate (4P4NX7) is between the electrodes. Nonetheless, 12 plates have been set as neutral plates in Configuration-3 named 1P2NX12, as shown in Fig. 2. In this study, P represents positive, N represents negative, and X represents neutral. The electrolyzer's performance was measured using a 14VDC power source with a capacity of 100 A to supply the electrolysis power. The voltage output is controlled using pulse width modulation (PWM). A voltmeter was connected in parallel to the PWM output to measure the voltage, and an ammeter was attached in series to measure the current. A K-type thermocouple was used to measure the temperature of the electrolyte, and an air rotameter was used to measure the gas flow during the experimental process. The safety and reliability of the experimental setup are guaranteed by the bubbler and flashback arrestor, as illustrated in Fig. 2, where this experimental setup is shown to be in high compliance with safety standards. Not only does this new approach save time and effort when it comes to accurately measuring the changes in current in the system, but it also gives one the ability to fine-tune the voltages needed for the system to work as it should. The PWM technology and measuring equipment utilized enabled the level of efficiency and accuracy to be achieved, and these also will allow for a systematic understanding of its operational performance. Subramanian[33] comprehensively described the principles and mathematical models of the electrolysis process of water.

$$4H_2O + 4e^- \rightarrow 2H_2 + 4OH^- \text{ anode reaction} \quad (1)$$

$$4OH^- \rightarrow O_2 + 2H_2O + 4e^- \text{ cathode reaction} \quad (2)$$

The exposed surface area in the electrolyte is calculated using eqn (3). The calculated area is used to measure the current density.

$$A = 2\left(\frac{1}{2}b_1h_1\right) + b_2h_2 + b_3h_3 - N_h\left(\frac{\pi}{4}d^2\right)$$
$$= b_1h_1 + b_2h_2 + b_3h_3 - N_h\left(\frac{\pi}{4}d^2\right) = 142.42 \text{ cm}^2 \quad (3)$$

The current density is calculated using eqn (4)

$$J = \frac{I}{2AN_e} \quad (4)$$

J reflects the current density in A cm^{-2}, I represents the current flowing in Ampere (A), A represents the exposed electrode area

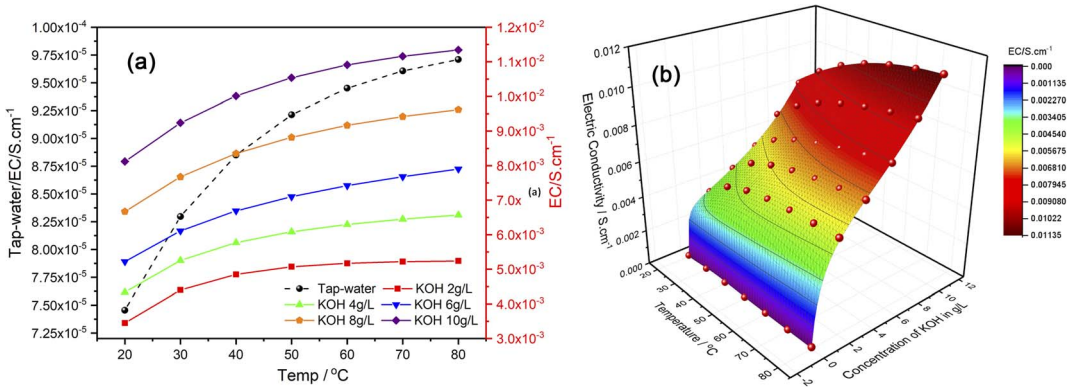

Fig. 3 Effect of temperature on water and electrolyte electric conductivity.

in the electrolyte, N_e is the number of electrodes and 2 reflects the sides of the electrodes exposed to the electrolyte.

It is essential to carefully measure an electrolyzer's critical variables to evaluate its performance. A variety of instruments, such as voltmeter, ammeter, thermocouple, timer, electronic balance, and gas flow meter, are used in this process. The accuracy of the data provided by these instruments is essential for evaluating the effectiveness and operation of the electrolyzer. The ranges and uncertainties of each instrument are documented to ensure measurement accuracy, as shown in Table 2.

The overall uncertainty of the experiment was calculated using eqn (5).

$$\mathrm{OE_{Un}} = \sqrt{(u_T)^2 + (u_t)^2 + (u_V)^2 + (u_A)^2 + (u_C)^2 + (u_Q)^2} \quad (5)$$

where u_T = uncertainty in electrolyte temperature, u_t = uncertainty in production time, u_V = uncertainty in applied voltage, u_A = uncertainty in applied current, u_C = uncertainty in electrolyte concentration, u_Q = uncertainty in gas flow rate

$$\mathrm{OE_{Un}} = \sqrt{(0.75)^2 + (0.1)^2 + (0.2)^2 + (0.2)^2 + (0.1)^2 + (5)^2} = \pm 5.066\% \quad (6)$$

3. Results and discussion

This study uses three electrode configurations to assess the performance across varied conditions in a constructed HHO cell. The focus has been testing the electrolyzer with three different concentrations of KOH electrolyte, specifically at 2 g L^{-1}, 4 g L^{-1}, and 6 g L^{-1}, to understand its comparative efficacy against water. A critical examination has been carried out on several parameters, including electric conductivity, HHO production at variable voltages, and the impact of electrolyte temperature on HHO production.

Electrode stability is another major issue for HHO electrolyzer efficiency, requiring further study. The following sections discuss how the electrolyte composition, electrode arrangement, and temperature impact the HHO production efficiency and stability.

3.1 Electrical conductivity evaluation of prepared electrolytes at different operating temperatures

Several studies have examined how the electrical conductivity of water affects the production of HHO gas, which contains hydrogen and oxygen from water electrolysis. These studies show water conductivity affects the HHO gas generation efficiency.[32] Water electrical conductivity rises with temperature. Water molecules have higher mobility at higher temperatures, which increases ionization and solution ion concentration. This study examined how altering the temperature and electrolyte content improved the electrical conductivity of water. As shown in Fig. 3a, there is a noticeable improvement in electrical conductivity due to temperature changes and variations in electrolyte concentration. This study reveals that the rate of change in electrical conductivity from 20 to 50 °C is significant. Meanwhile, fractional changes in conductivity are observed at temperatures above 60 °C with a concentration of 2 g L^{-1}. Similarly, fractional changes in electrical conductivity are evident at concentrations of 4, 6, and 8 g L^{-1}. However, at a concentration of 10 g L^{-1}, a notable improvement in electrical conductivity is seen up to 40 °C, after which only fractional changes are observed. The EC results obtained from this study are used to develop a mathematical model to predict electrical conductivity as a function of temperature and concentration of electrolyte (KOH) used in this study. The 3D surface fitting method was used to develop a surface that represents the set of data in three-dimensional space, as shown in Fig. 3b.

The Rational Taylor model was used to develop the EC prediction mathematical model as given in eqn (7) using experimental data.

$$\mathrm{EC} = \frac{-1.98E-5 + 1.085E-6x + 0.00495y + 3.177E-4y^2 + 1.698E-4x \times y}{1 - 0.055x + 2.53y + 8.67E-4x^2 - 0.128y^2 + 0.00571xy} \quad (7)$$

In this model, the value of x is the temperature in °C, whereas y is the mass value of the electrolyte in g L^{-1}. This Rational Taylor model provides the best fit from experimental data, where the value of R-square is 0.998. The developed model from this study provides approximately equal results of EC at variable temperatures from 20 to 80 °C and 0 to 10 g L^{-1} of KOH concentration.

3.2 Evaluation of HHO gas production at variable voltages

Voltage plays a critical role in the operation of HHO generators because it directly impacts the control, safety, efficiency, and gas production rate of the device. In this research, voltage control was achieved through PWM (Pulse Width Modulation), and extensive testing was conducted on three different HHO generator configurations. As depicted in Fig. 4a, it is evident that with the increasing PWM percentage and voltage, the HHO production response also shows a corresponding increase. Upon closer examination of the graph, it becomes apparent that the HHO production rate remains consistently high, up to 60% PWM, producing HHO at rates ranging from 0.1 to 0.4 L min^{-1} for 2 g L^{-1} concentration, from 0.38 to 0.56 L min^{-1} for 4 g L^{-1} concentration, and from 0.7 to 0.95 L min^{-1} for 6 g L^{-1} concentration of the electrolyte. However, beyond the 60% PWM rate, the hydrogen production rate is reduced. This is

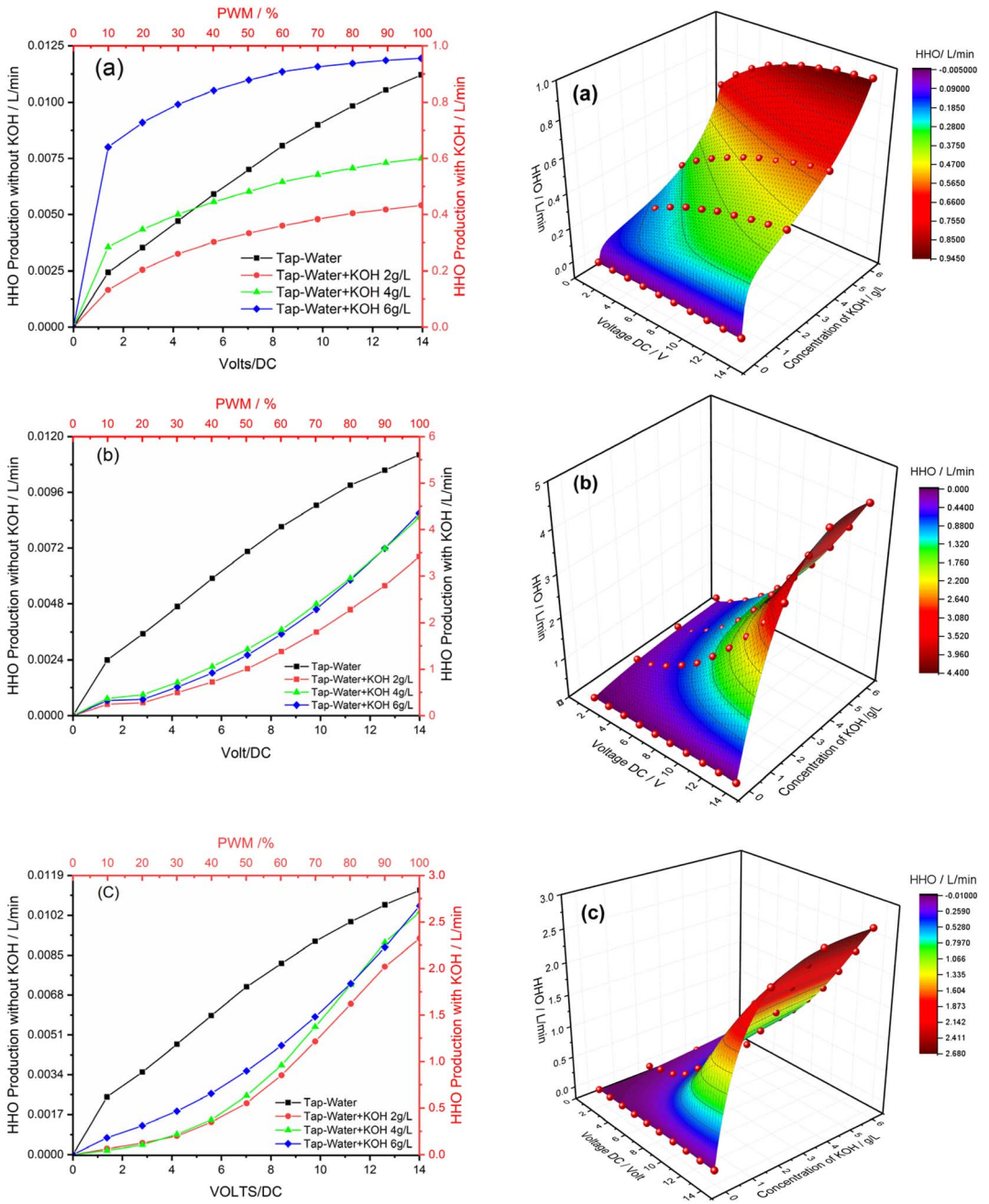

Fig. 4 Effect of voltage in oxyhydrogen gas production using PWM. (a) Configuration 1, (b) Configuration 2 and (c) Configuration 3.

Table 3 Fitted parameters for the prediction of HHO gas production at different voltages and KOH concentrations

		Values of the fitted model from experimental data		
Sr.	Fitting parameters	Configuration-1	Configuration-2	Configuration-3
1	*X*-value	Applied voltage to predict HHO production	Applied voltage to predict HHO production	Applied voltage to predict HHO production
2	*Y*-value	Concentration of KOH in g L^{-1}	Concentration of KOH in g L^{-1}	Concentration of KOH in g L^{-1}
3	Z_0	-0.00115 ± 0.00399	0.0052 ± 0.0139	0.00374 ± 0.00929
4	A_{01}	$5.071 \times 10^{-4} \pm 7.731 \times 10^{-4}$	$-2.7105 \times 10^{-4} \pm 0.0012$	$-2.5502 \times 10^{-4} \pm 8.0463 \times 10^{-4}$
5	B_{01}	0.50748 ± 0.31678	0.05689 ± 0.02062	-0.05995 ± 0.03353
6	B_{02}	0.03495 ± 0.03372	-0.00341 ± 0.00393	0.01464 ± 0.00649
7	C_{02}	0.17368 ± 0.13026	0.032 ± 0.00503	0.02332 ± 0.00566
8	A_1	-0.22412 ± 0.09438	-0.11488 ± 0.00519	-0.16044 ± 0.00878
9	A_2	0.01646 ± 0.01015	$0.00411 \pm 3.1283 \times 10^{-4}$	$0.0068 \pm 6.51784 \times 10^{-4}$
10	B_1	6.06092 ± 4.44762	0.11954 ± 0.02563	0.20951 ± 0.06154
11	B_2	-0.81346 ± 0.5853	0.0078 ± 0.00212	0.00827 ± 0.00364
12	C_2	0.14083 ± 0.0968	-0.00622 ± 0.00177	-0.01014 ± 0.0037
13	Reduced Chi-sqr	7.05909×10^{-5}	0.00154	0.00234
14	*R*-square (COD)	0.99947	0.99933	0.99761
15	Adj. *R*-square	0.99931	0.99913	0.9969

because no neutral plate has been incorporated, and an equal voltage has been applied to electrodes in this configuration.

Fig. 4b shows a clear trend indicating that as the percentage of PWM increases, hydrogen production also increases. However, it is noteworthy that the production rate significantly escalates after reaching 70% of PWM. The primary reason behind this phenomenon can be attributed to the introduction of a neutral plate between the cathode and anode in Configuration 2. This modification divides 9.8 volts, corresponding to 70% PWM, into two halves, effectively supplying 4.9 volts to each cell. Furthermore, Fig. 4b also reveals the minimal difference in hydrogen production between 4 and 6 g L^{-1} concentrations. Conversely, a concentration of 2 g L^{-1} of the electrolyte produces approximately 20% less hydrogen than the 4 and 6 g L^{-1} concentrations, highlighting the impact of electrolyte concentration on hydrogen production efficiency. In Configuration 3, six neutral plates have been utilized between the electrodes. This arrangement reduced the production by approximately 39% compared to Configuration 2, especially at 4 and 6 g L^{-1} concentrations. Furthermore, there has been a 31.4% decrease in HHO production at 2 g L^{-1}, as illustrated in Fig. 4c.

There has been limited literature on models for predicting HHO production. Therefore, this study developed a mathematical model to predict HHO production at any value in the range of 1 to 14 VDC applied voltages and 0 to 6 g L^{-1} of KOH concentration. The model developed for HHO production in this study is based on experimental data extracted during the experiment and uses a nonlinear surface model to develop the HHO production model, as shown in eqn (8). In this model, x represents the applied voltage at which HHO production should be predicted, and y represents the KOH concentration in g L^{-1}. The parameters Z_0 to C_2 are empirical constants, and their values are given in Table 3. The R^2 value for the developed model for HHO production is 0.99, which indicates its high accuracy, as mentioned in Table 3.

3D surface nonlinear fitted model for HHO dry cell generator to predict HHO production.

$$\text{HHO production} = \frac{(Z_0 + A_{01} \times x + B_{01} \times y - B_{02} \times y^2 + C_{02} \times x \times y)}{(1 + A_1 \times x + B_1 \times y + A_2 \times x^2 + B_2 \times y^2 + C_2 \times x \times y)} \quad (8)$$

3.3 Effect of electrolyte temperature on HHO gas production

Temperature substantially affects the production of oxyhydrogen in HHO generators, influencing the amount of gas generated and the efficiency of the electrolysis process. In this study, the experiments were carried out in a controlled environment, as depicted in Fig. 5a–c. The temperature of the electrolyte at the start of the experiment was 25 °C, which gradually increased over time. All the investigations were carried out with 100% PWM, equal to 14 VDC. Fig. 5a shows that the most significant rise in electrolyte temperature occurred in the solution with a concentration of 6 g L^{-1}. Concurrently, the production of hydrogen gas peaked during the first 20 minutes, then consistently decreased. In contrast, the solutions with 2 g L^{-1} and 4 g L^{-1} concentrations exhibited a consistent increase in temperature with respect to time. As the electric current passes through the electrolyte solution, it encounters resistance. This resistance is not constant and can increase as the concentration of ions changes due to the ongoing electrolysis. The resistance to electric current generates heat analogous to how a wire heats up when it carries a current.

In actuality, pure water is a poor electrical conductor. An important factor contributing to the conductivity of water is the presence of dissolved ions. These ions become less mobile and are less available in the solution as corrosion products are generated by encasing or consuming them. This lowers the water's conductivity. In water, this process can lead to the formation of corrosion products, such as rust (iron oxides) in the case of iron or steel. As in this study, these products can be solid particulates that do not dissolve well in water, producing higher resistance in electrolyte solutions, improving heat generation, and reducing gas production. However, in Configuration 2, there is a higher consistency in

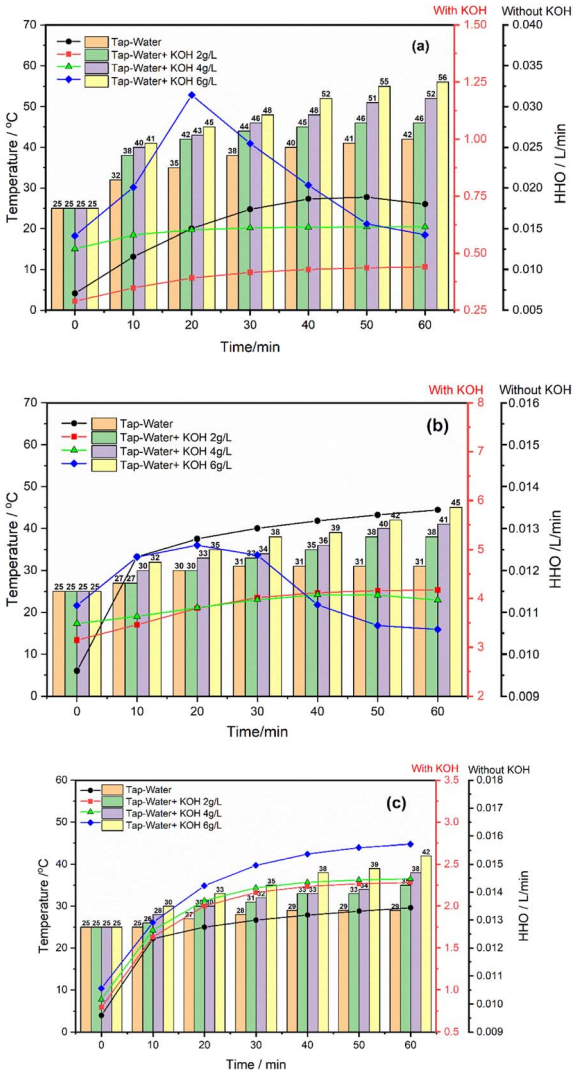

Fig. 5 Variation in HHO gas production and electrolyte temperature with respect to time: (a) Configuration-1; (b) Configuration-2; (c) Configuration-3.

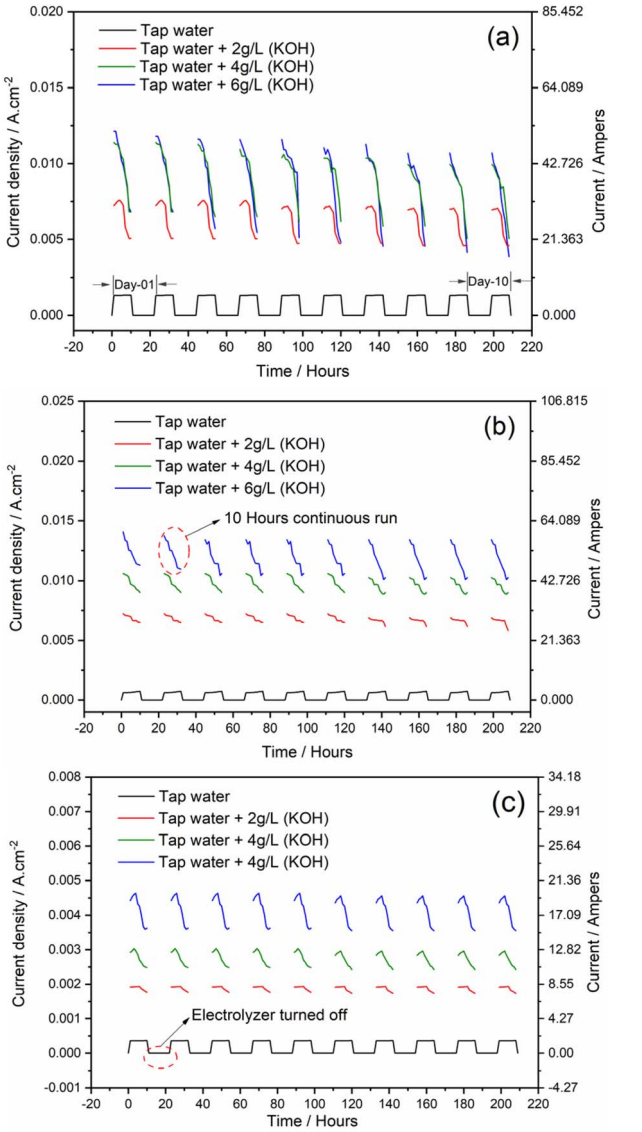

Fig. 6 Current density and energy consumption evaluation on a long run of HHO generator: (a) Configuration-1, (b) Configuration-2, and (c) Configuration-3.

HHO production, which is approximately 4 L min^{-1} at both 2 g L^{-1} and 4 g L^{-1} concentrations when compared to Configurations 1 and 3. Meanwhile, at a concentration of 6 g L^{-1}, after 20 minutes of operation, the production of oxyhydrogen gas consistently decreased. It is because each cell in the stack runs on 6.9 volts, which is determined by a voltmeter. As observed in this study, in Configuration 3, there is a gradual increase in both temperature and gas production. This can be attributed to the increased number of neutral plates in Configuration 3. Adding more neutral plates facilitates a gradual transfer of ions, resulting in a slower production process and a gradual rise in temperature.

3.4 Stability investigation of HHO generator electrodes for long-term runs

Efficient and stable electrodes are crucial for the practical applications of hydrogen generators. Research into various electrolyte concentrations and configurations aims to reduce the overpotentials required for the desired current densities, enhance long-term stability, and facilitate the integration of these electrodes into commercial devices. In this study, the stability of electrodes has been investigated. To measure the stability of electrodes, a generator was run continuously at a constant 14 volts for 10 hours. After this period, the generator was stopped for 10 hours, after which the generator was run again for 10 hours using the same method for 10 days. After 10 days of continuous operation, the generator was disassembled, and the electrodes were examined through microscopic testing. It was observed that the current density consistently decreased in Configuration 1 and 6 g L^{-1} concentration. Initially, there was a reduction in current density, which amounted to 43% at the end of 10 hours. Similarly, upon completing the ten days, the current density increased, reaching a reduction of 65%, as shown in Fig. 6a. The primary cause of the decrease in current density was identified as the production of iron oxide during the electrolysis process,

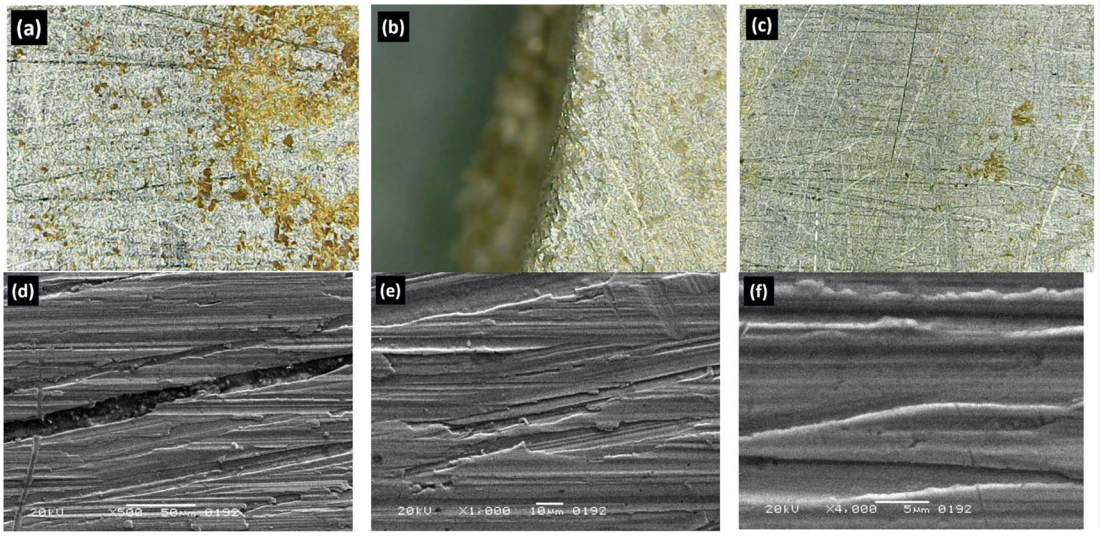

Fig. 7 Digital microscopic and SEM images of different locations of electrodes run on Configuration-1, 6 g L^{-1}, after a 10 days run in the HHO generator. Figure (a), (b) and (c) are microscopic images, figure (d), (e) and (f) are SEM images.

which reduced the conductivity of the water-electrolyte solution. This study also revealed that a concentration of 2 g L^{-1} resulted in higher current density stability in Configurations 2 and 3. Furthermore, it can be observed that the current density in Configuration 2 is 73% higher than that in Configuration 3 at a concentration of 2 g L^{-1}, as shown in Fig. 6b. In this study, it was found that current stability ensures that the electrolysis process remains consistent and prevents fluctuations in gas production, with the constant current flow reducing energy loss. This ensures that the maximum amount of electrical energy is converted into chemical energy (HHO gas), which improves the overall energy efficiency.

In this research, it has been observed that in Configuration 1, with higher current density and an electrolyte concentration of 6 g L^{-1}, there is a consistent decrease in current density over a 10 hours run. The fundamental reason for this phenomenon is the formation and deposition of iron oxide on electrodes due to excessive current passing through the electrolyte, as illustrated in Fig. 7. The formed iron oxide is deposited on the surface of the electrode; however, no electrode degradation was seen in this study, as shown in Fig. 7. A key concept in iron oxide production is the electrochemical behaviour of iron electrodes in alkaline solutions, such as KOH. This study also reveals that stable current reduces wear and tear on the electrodes and also prevents excessive heat or abnormal electrochemical reactions that may cause the electrode to deteriorate. This will extend the life of the generator and reduce maintenance costs.

4. Conclusion

In this research, the electrolyzer was designed in three distinct configurations. A gap of 4 mm was maintained between each electrode using rubber spacers. In Configuration 1, no neutral plate was used between the cathode and anode. In contrast, Configuration 2 incorporated a neutral plate between the cathode and anode, and similarly, Configuration 3 involved the placement of four plates between the cathode and anode. All three configurations were tested at 2, 4, and 6 g per L KOH concentrations. It was observed that in Configuration 1, the gas production initially increased consistently, which, after 20 minutes of operation, began to decrease when the electrolyte concentration was 6 g L^{-1}. This phenomenon was primarily attributed to the formation of iron oxide due to higher current densities and applied voltages, leading to a decrease in water conductivity. Consequently, a consistent reduction in current density was observed over a long-term operation of 10 hours, resulting in a 43% reduction on the first day, which further escalated to a 65% reduction by the tenth day. The study also found that Configurations 2 and 3 exhibited better current density stability at a concentration of 2 g L^{-1}. When comparing these two configurations, Configuration 2 showed superior results with approximately consistent gas production rates of about 4.2 L min^{-1}. The stable current ensures efficient use of electricity, which reduces the overall energy costs of the gas production process. This is especially important for large operations where significant energy savings can be achieved.

Data availability

The essential data supporting this article have been included as part of the ESI.†

Conflicts of interest

There are no conflicts to declare.

Acknowledgements

We extend our sincere gratitude to the subsequent financing sources: National Natural Science Foundation of China (Grant

No. 52279036), The Key R&D Program Project of Jiangsu Province (Grant No. BE2021341) and Jiangsu Postdoctoral Excellent Program under Grant No. 2024ZB886. The authors gratefully acknowledge the financial support provided, which made this study possible.

References

1 H. Stančin, *et al.*, A review on alternative fuels in future energy system, *Renewable Sustainable Energy Rev.*, 2020, **128**, 109927.
2 Air, I., *World Air Quality Report. Region & City PM2*, 2019, p. 5.
3 B. Subramanian and V. Thangavel, Analysis of onsite HHO gas generation system, *Int. J. Hydrogen Energy*, 2020, **45**(28), 14218–14231.
4 L.-F. Chen, *et al.*, Uniformly bimetal-decorated holey carbon nanorods derived from metal–organic framework for efficient hydrogen evolution, *Sci. Bull.*, 2021, **66**(2), 170–178.
5 F. Ursino, *et al.*, Processing of molybdenum industrial waste into sustainable and efficient nanocatalysts for water electrolysis reactions, *Nano Res.*, 2024, **17**(11), 9585–9593.
6 J. Hansen, *et al.*, Global warming in the twenty-first century: An alternative scenario, *Proc. Natl. Acad. Sci. U. S. A.*, 2000, **97**(18), 9875–9880.
7 B. Subramanian and V. Thangavel, Experimental investigations on performance, emission and combustion characteristics of Diesel-Hydrogen and Diesel-HHO gas in a Dual fuel CI engine, *Int. J. Hydrogen Energy*, 2020, **45**(46), 25479–25492.
8 A. A. Al-Rousan, Reduction of fuel consumption in gasoline engines by introducing HHO gas into intake manifold, *Int. J. Hydrogen Energy*, 2010, **35**(23), 12930–12935.
9 M. S. Kumar, A. Ramesh and B. Nagalingam, Use of hydrogen to enhance the performance of a vegetable oil fuelled compression ignition engine, *Int. J. Hydrogen Energy*, 2003, **28**(10), 1143–1154.
10 J. W. Heffel, NOx emission and performance data for a hydrogen fueled internal combustion engine at 1500rpm using exhaust gas recirculation, *Int. J. Hydrogen Energy*, 2003, **28**(8), 901–908.
11 W. Liao, *et al.*, Application of in situ/operando characterization techniques in heterostructure catalysts toward water electrolysis, *Nano Res.*, 2023, **16**(2), 1984–1991.
12 R. M. Santilli, A new gaseous and combustible form of water, *Int. J. Hydrogen Energy*, 2006, **31**(9), 1113–1128.
13 J. Olivares-Ramírez, *et al.*, Studies on the hydrogen evolution reaction on different stainless steels, *Int. J. Hydrogen Energy*, 2007, **32**(15), 3170–3173.
14 A. C. Yilmaz, E. Uludamar and K. Aydin, Effect of hydroxy (HHO) gas addition on performance and exhaust emissions in compression ignition engines, *Int. J. Hydrogen Energy*, 2010, **35**(20), 11366–11372.
15 T. Arjun, *et al.*, A review on analysis of HHO gas in IC engines, *Mater. Today: Proc.*, 2019, **11**, 1117–1129.
16 S. e. A. Musmar and A. A. Al-Rousan, Effect of HHO gas on combustion emissions in gasoline engines, *Fuel*, 2011, **90**(10), 3066–3070.
17 B. Sudarmanta, S. Darsopuspito and D. Sungkono, Application of dry cell HHO gas generator with pulse width modulation on sinjai spark ignition engine performance, *Int. J. Res. Eng. Technol.*, 2016, **5**(2), 105–112.
18 T. De Silva, L. Senevirathne and T. Warnasooriya, HHO generator–an approach to increase fuel efficiency in spark ignition engines, *Eur. J. Adv. Eng. Technol.*, 2015, **2**(4), 1–7.
19 K. Mazloomi, N. B. Sulaiman and H. Moayedi, Electrical efficiency of electrolytic hydrogen production, *Int. J. Electrochem. Sci.*, 2012, **7**(4), 3314–3326.
20 Y. M. Shashikant and S. S. Maruti, Parametric study on Oxy hydrogen gas generation and associated energy consumption using Taguchi's design of experiment concept, in *2017 International Conference on Nascent Technologies in Engineering (ICNTE)*, IEEE, 2017.
21 A. Bahlake, F. Bahlake and A. Mirabi, Electrolyte and temperature optimization of electrochemical cells using design of expriments (DOE), *Adv. Appl. Sci. Res.*, 2012, **3**(4), 2235–2242.
22 P. Polverino, *et al.*, Study of the energetic needs for the on-board production of Oxy-Hydrogen as fuel additive in internal combustion engines, *Energy Convers. Manage.*, 2019, **179**, 114–131.
23 H. Masjuki, *et al.*, Study of production optimization and effect of hydroxyl gas on a CI engine performance and emission fueled with biodiesel blends, *Int. J. Hydrogen Energy*, 2016, **41**(33), 14519–14528.
24 A. A. Al-Rousan and A. Sa'ed, Effect of anodes-cathodes inter-distances of HHO fuel cell on gasoline engine performance operating by a blend of HHO, *Int. J. Hydrogen Energy*, 2018, **43**(41), 19213–19221.
25 I. Elgarhi, M. M. El-Kassaby and Y. A. Eldrainy, Enhancing compression ignition engine performance using biodiesel/diesel blends and HHO gas, *Int. J. Hydrogen Energy*, 2020, **45**(46), 25409–25425.
26 M. El Kady, *et al.*, Parametric study and experimental investigation of hydroxy (HHO) production using dry cell, *Fuel*, 2020, **282**, 118825.
27 N. Alam and K. Pandey, Experimental study of hydroxy gas (HHO) production with variation in current, voltage and electrolyte concentration, in *IOP Conference Series: Materials Science and Engineering*, IOP Publishing, 2017.
28 A. K. El Soly, M. Gad and M. El Kady, Experimental comparison of oxyhydrogen production rate using different designs of electrolyzers, *Int. J. Hydrogen Energy*, 2023, **48**(93), 36254–36270.
29 M. Gad and A. El Soly, Improvements of combustion, emissions and exergy in petrol engine using oxyhydrogen from different configurations, *Int. J. Hydrogen Energy*, 2024, **49**, 1020–1032.
30 M. Gad, *et al.*, Impact of produced oxyhydrogen gas (HHO) from dry cell electrolyzer on spark ignition engine characteristics, *Int. J. Hydrogen Energy*, 2024, **49**, 553–563.
31 A. Rashad and A. Elmaihy, Theoretical and experimental performance of oxy-hydrogen generators, *Arabian J. Sci. Eng.*, 2018, **43**, 1279–1289.

32 M. Streblau, *et al.*, The influence of the electrolyte parameters on the efficiency of the oxyhydrogen (HHO) generator, in *2014 18th International Symposium on Electrical Apparatus and Technologies (SIELA)*, 2014.

33 B. Subramanian, Production and use of HHO gas in IC engines, *Int. J. Hydrogen Energy*, 2018, **43**(14), 7140–7154.